Transition conditions at the interface between floating plates

Hyuck Chung* and Colin Fox†

1 Introduction

This paper presents a Wiener-Hopf (W-H) solution of wave propagation across a crack where two semi-infinite floating elastic plates are joined by various transition conditions (see Fig. 1). There has been a steady development of analytical solutions of floating elastic plates and water waves. A simple case of water-plate interaction problem is solved in [1] and [4] using the W-H technique. (There are too many papers on the W-H to list them all here.) A similar technique is used in [3] to solve a plate-plate interaction with an open gap and a rigid joint. In a slightly different situation, [2] gives analytical solutions of plate-water-plate problem using the residue calculus technique. A complementary problem, water-plate-water with free edge conditions is solved using the W-H in [7]. Wave scattering by a long crack is studied in [5] using a Green's function for a floating elastic plate. The family of problems concerning floating elastic plates, which can be solved analytically, is growing and several of them have been presented at the past workshops. However, the conditions at the edges of the plates have been usually assumed to be free. In this paper we exploit the fact that the W-H technique can, with some modifications shown in [3], incorporate more complex transition conditions than the simple open gap or rigid joint.

Our motivation here is to model the cracks in sea-ice sheets, because wave propagation into the ice field plays an important role when the ice sheets around the coast of Antarctica are broken up every year. We use a theoretical model of the ice sheet that assumes ice thickness, mass density and Young's modulus to be constant. This model is often used to study the dynamics of ice sheets with fairly homogeneous appearance. We focus on a relatively long and straight crack in an ice sheet. Such a crack can have a variety of physical properties depending on how it is formed, for example partially frozen slosh or solidly re-frozen crack. However, the mechanism of wave propagation across such a crack is not yet well understood.

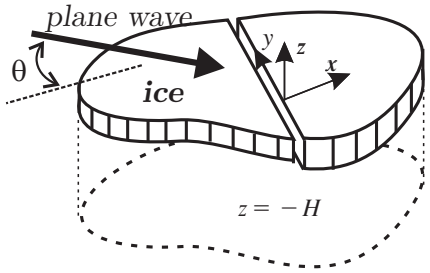

Figure 1: Schematic drawing of the crack in an ice sheet.

In order to model varying characteristics of the crack, we introduce theoretical transition conditions using two springs linking the ice sheets (see Fig. 2). The vertical spring transmits the shear force that is determined by the displacement difference. The rotational spring transmits the bending moment that is determined by the difference of the gradient at the edges of the ice sheets.

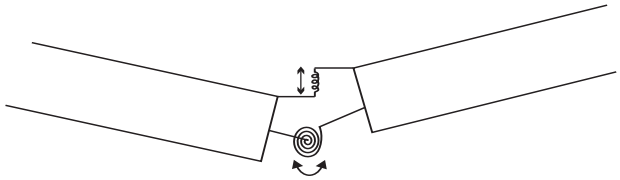

Figure 2: The rotational and the vertical springs connecting the two ice sheets.

The solutions here are given as an expansion over the modes that exist in ice sheets. The coefficients of the expansion are linear combination of four constants that must be determined by the transition conditions.

*Acoustics Research Centre, School of Architecture, University of Auckland, PB 92019 Auckland, New Zealand, hyuck@math.auckland.ac.nz

†Department of Mathematics, University of Auckland, PB 92019 Auckland, New Zealand, fox@math.auckland.ac.nz

Although, the W-H technique has been used by several researchers, its strength, which is the simple use of the transition conditions, has not been exploited. From the transition conditions a system of equations for the constants can be formulated with a 4×4 matrix and a vector. We therefore focus on the formulation of the matrix and the vector to study the qualitative behaviour of the solutions.

2 Governing equations

The displacement, $w(x,y,t)$, and the velocity potential of the water, $\phi(x,y,z,t)$, satisfy the following system of equations.

$$\left.\begin{array}{c} p = D_1\nabla^4_{x,y}w + m_1\left(w_{tt}+g\right),\ \text{for } x<0,\\ p = D_2\nabla^4_{x,y}w + m_2\left(w_{tt}+g\right),\ \text{for } x>0,\\ w_t = \phi_z,\\ \rho\phi_t + \rho g w + p = 0,\\ \phi_z = 0 \quad \text{at } z=-H,\\ \nabla^2_{x,y,z}\phi = 0 \text{ in the water.} \end{array}\right\} \text{at } z=0 \tag{2.1}$$

g, ρ and p are acceleration due to the gravity, mass density of sea water and pressure acted on the surface of the water respectively. The mass density of each plate is denoted by $m_i = \rho_i h_i$ (ρ_i is the mass density of the ice, h_i is the thickness), $i=1,2$ respectively. D_i, $i=1,2$ are the flexural rigidity of the ice sheets. We assume that there exists an incoming plane wave obliquely incident from infinite that is harmonic in time, that is, at $x=-\infty$ we have $\mathrm{i}\,I\exp\mathrm{i}\left(\lambda x+\omega t\right)$, where I is amplitude of the wave (i is there to simplify the calculations in the Wiener-hopf technique) and the wave number λ is determined by the incident angle of the plane wave to the x-axis. Since the system of the equations 2.1 are linear with respect to $\phi(x,y,z,t)$, we may express the solution as

$$\phi(x,y,z,t) = \mathrm{Re}\left[\phi(x,z,\omega)\,e^{\mathrm{i}(ky+\omega t)}\right]$$

where $\phi(x,z,\omega)$ (or $\phi(x,z)$ for simplicity) is the complex function of amplitude of the solution and k denotes the wave number in the y-axis, i.e., $k=\lambda'\sin\theta$, $\lambda'=\sqrt{\lambda^2+k^2}$ and θ being the incident angle as depicted in Fig. 1.

We scale (or non-dimensionalize) the system of equations given above using characteristic length and characteristic time denoted by l_i and t_i, $i=1,2$ respectively. The subscript $i=1$ corresponds to the plate for $x<0$ and $i=2$ for $x>0$ and characteristic length, characteristic time and the ratio of the characteristic lengths are defined as

$$l_i = \left(\frac{D_i}{\rho g}\right)^{1/4},\ \ t_i = \sqrt{\frac{l_i}{g}},\ \ l_\mathrm{r} = \frac{l_1}{l_2}.$$

We here assume that $l_\mathrm{r}<1$, i.e., the plate on the right is more rigid than the other. l_r may be zero when $x<0$ is free-surface. If we denote the non-dimensional variables with the bar, then the non-dimensionalized variables of space and time using l_2 are

$$(\bar{x},\bar{y},\bar{z}) = \frac{1}{l_2}(x,y,z),\ \bar{t} = \frac{t}{t_2}.$$

We omit the bar to avoid the clutter from now.

3 Solutions using the Wiener-Hopf technique

This section shows the solutions of the system of equations 2.1 that are derived using the W-H technique. The detailed derivation of the solution is given in [3].

We derive scaled version of the reflection and transmission coefficients from the system of equations given by

$$\begin{array}{c} \left\{l_\mathrm{r}^4\left(\partial_x^2-k^2\right)^2 - m_1\omega^2+1\right\}\phi_z(x,0) = \omega^2\phi(x,0),\ x<0,\\ \left\{\left(\partial_x^2-k^2\right)^2 - m_2\omega^2+1\right\}\phi_z(x,0) = \omega^2\phi(x,0),\ x>0 \end{array} \tag{3.1}$$

We apply the Fourier transform to the differential equations of ϕ in the respective domains $x<0$ and $x>0$, which are defined as

$$\Phi_+(\alpha,z) = \int_0^\infty \phi(x,z)\,e^{\mathrm{i}\,\alpha x}dx,\ \ \Phi_-(\alpha,z) = \int_{-\infty}^0 \phi(x,z)\,e^{\mathrm{i}\,\alpha x}dx \tag{3.2}$$

where α is the complex variable and $\Phi_\pm$ are the complex valued functions. From 3.2 the Fourier transform of ϕ int he whole domain is $\Phi=\Phi_++\Phi_-$. The inverse Fourier transform is then defined as

$$\phi(x,0) = \frac{1}{2\pi}\int_{-\infty}^{\infty}\Phi(\alpha)\,e^{-\mathrm{i}\,\alpha x}\,d\alpha$$

where the integration path on the real axis is indented around the real singularities and may be closed in either the upper or lower half plane depending whether $x < 0$ or $x > 0$.

For $x < 0$ we close the integral contour in the upper half plane, and put the incident wave back, then we have

$$\begin{aligned} \phi_z(x,0) &= \mathrm{i} I e^{\mathrm{i}\lambda x} - \sum_{q\in S_1} \frac{\mathrm{i} F(q) q' R_1(q')}{qK(q)} e^{-\mathrm{i} qx}, \\ \phi(x,z) &= \frac{\mathrm{i} I \cosh\lambda'(z+H)}{\lambda' \sinh\lambda' H} e^{\mathrm{i}\lambda x} - \sum_{q\in S_1} \frac{\mathrm{i} F(q) R_1(q') \cosh q'(z+H)}{qK(q)\sinh q' H} e^{-\mathrm{i} qx} \end{aligned} \tag{3.3}$$

where $\lambda' = \sqrt{\lambda^2 + k^2}$ and

$$F(\alpha) = J(\alpha) - \frac{I f_2(\gamma)}{(\alpha+\lambda)K(\lambda)}, \quad J(\alpha) = d_0 + d_1\alpha + d_2\alpha^2 + d_3\alpha^3.$$

and

$$\begin{gathered} f_1(\gamma) = l_{\mathrm{r}}^4\gamma^4 - m_1\omega^2 + 1 - \tfrac{\omega^2}{\gamma\tanh\gamma H}, \quad f_2(\gamma) = \gamma^4 - m_2\omega^2 + 1 - \tfrac{\omega^2}{\gamma\tanh\gamma H}, \\ \tfrac{f_2}{f_1} = K(\alpha)K(-\alpha), \quad K(\alpha) = \left(\prod_{q=S_1} \tfrac{q'}{q+\alpha}\right)\left(\prod_{q=S_2} \tfrac{q+\alpha}{q'}\right). \end{gathered}$$

The sets of the modes are defined as

$$S_j = \left\{\alpha \in \mathbb{C} \mid f_j(\gamma(\alpha)) = 0,\ \alpha = \sqrt{\gamma^2 - k^2},\ \text{either } \operatorname{Im}\alpha > 0 \text{ or } \alpha > 0\right\}.$$

We indicate the roots of the dispersion functions, f_1 and f_2 corresponding to the elements of S_j by the prime, for example if $\lambda \in S_1$ then λ' on the γ-plane satisfies $f_1(\lambda') = 0$. Detailed descriptions of the roots are given in [6]. Residue function $R_1(q')$ of $[f_1(\gamma)]^{-1}$ at $\gamma = q'$ is

$$R_1(q') = \left(\left.\tfrac{df_1(\gamma)}{d\gamma}\right|_{\gamma=q'}\right)^{-1} = \tfrac{\omega^2 q'}{(5l_{\mathrm{r}}^4 q'^4 + b_1)\omega^2 + H\left((l_{\mathrm{r}}^4 q'^5 + b_1 q)^2 - \omega^4\right)}. \tag{3.4}$$

We used $b_1 = -m_1\omega^2 + 1$ and $f_1(q') = 0$ to simplify the formula. Displacement $w(x)$ can be obtained by multiplying $-\mathrm{i}/\omega$ to equation 3.3.

For $x > 0$, we derive $\phi_z(x,0)$ then $\phi(x,z)$ by closing the integral contour in the lower half plane,

$$\begin{aligned} \phi_z(x,0) &= -\sum_{q\in S_2} \frac{\mathrm{i} K(q) F(-q) q' R_2(q')}{q} e^{\mathrm{i} qx}, \\ \phi(x,z) &= -\sum_{q\in S_2} \frac{\mathrm{i} K(q) F(-q) R_2(q') \cosh q'(z+H)}{q\sinh q' H} e^{\mathrm{i} qx}, \end{aligned} \tag{3.5}$$

where R_2 is a residue of $[f_2(\gamma)]^{-1}$ and its formula can be obtained by replacing the subscript 1 with 2 and l_{r} with 1 in equation 3.4.

4 Transition conditions

We consider here the case when $l_{\mathrm{r}} = 1$ and the incident angle is zero. Fig. 3 shows the reflection coefficient as a function of the two spring constants at different incident wave frequencies. There is little reflection of waves when τ_1 and τ_2 are large as the transition is very rigid. The equations for the transition conditions depicted in Fig. 2 are

$$\begin{aligned} B_1 w|_{x=0-} = B_1 w|_{x=0+} \quad &, \quad B_2 w|_{x=0-} = B_2 w|_{x=0+}, \\ \tau_1\left(w|_{x=0-} - w|_{x=0+}\right) = \pm B_1 w|_{x=0\pm} \quad &, \quad \tau_2\left(w_x|_{x=0-} - w_x|_{x=0+}\right) = \pm B_2 w|_{x=0\pm}, \end{aligned}$$

where τ_1 and τ_2 are the vertical and the rotational spring constants, respectively. The shear force and the bending moment are defined as

$$\begin{aligned} B_1 w|_{x=0+} = w_{xxx} - k^2(2-\nu) w_x \quad &, \quad B_1 w|_{x=0-} = l_{\mathrm{r}}^4\left\{w_{xxx} - k^2(2-\nu) w_x\right\}, \\ B_2 w|_{x=0+} = w_{xx} - k^2\nu w \quad &, \quad B_2 w|_{x=0-} = l_{\mathrm{r}}^4\left(w_{xx} - k^2\nu w\right) \end{aligned}$$

When $\tau_1 \to 0$ or/and $\tau_2 \to 0$, the transition conditions are equivalent to a clamped or roller connection, or an open gap. Similarly, when $\tau_1 \to \infty$ and $\tau_2 \to \infty$, the transition conditions become continuously joined. The above system of equations can be simply written using a matrix and a vector,

$$\mathcal{T}\mathbf{d} = \mathbf{v} \tag{4.1}$$

where $\mathbf{d} = (d_0, d_1, d_2, d_3)$ (column vector).

At a low frequency range the variation of the transitions conditions makes little difference to the wave propagation. Fig. 4 shows 4 singular values of $\mathcal{T}$. The figures show that the transition matrix stays virtually unchanged for $\omega < 0.7$ regardless of varying spring constants. Fig. 3 shows that the vertical and the rotational springs are equally influential to the reflection of the waves. However, the vertical spring induces more rapid variation to the reflection.

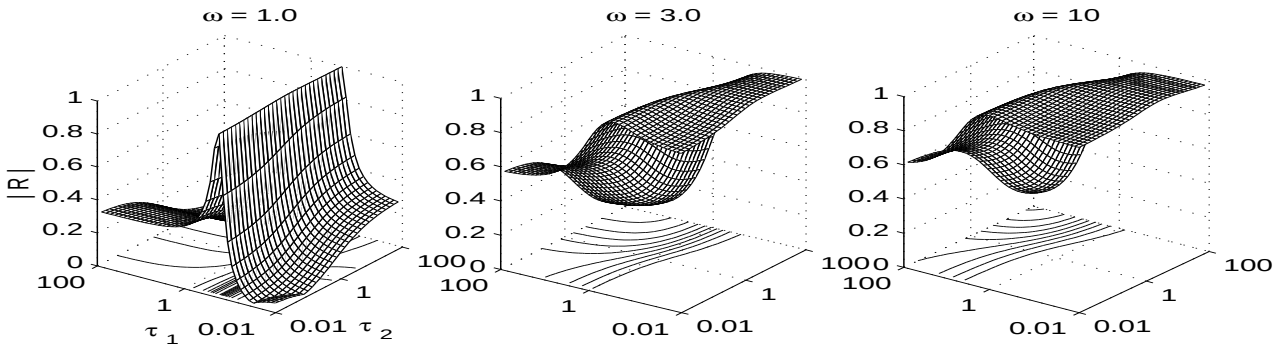

Figure 3: The reflection coefficients and the spring constants. The axes τ_1 and τ_2 are in log-scale.

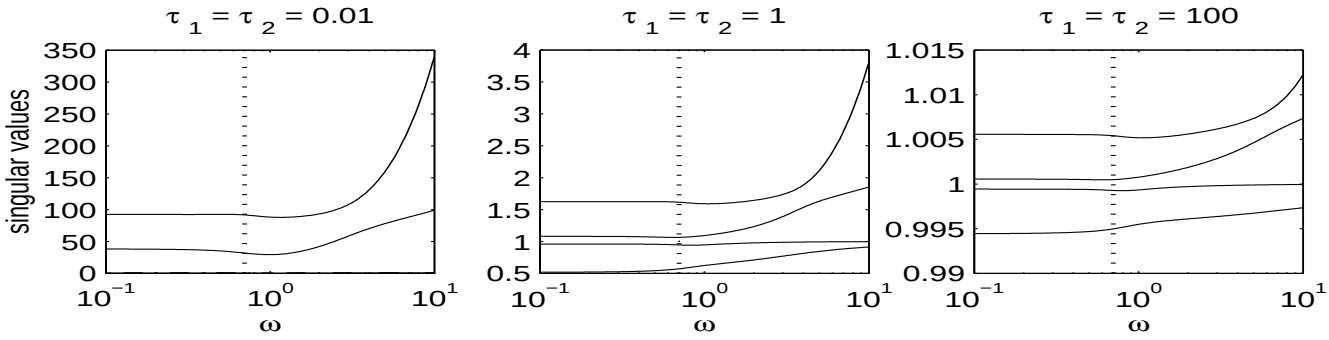

Figure 4: The singular values of $\mathcal{T}$ versus frequency ω for various spring constants. The dotted line is at $\omega = 0.7$.

5 Conclusions

This paper gives an initial attempt at modelling the transition conditions in an ice sheet. The conditions are reduced to the vertical and the rotational springs. Further studies and field measurements must be conducted to find the correlation between the theoretical model here and the real transition in an ice sheet. The fact that the solution by the W-H technique has explicit formulae (invariant to the transition conditions) for the coefficients of d_0, d_1, d_2, d_3 is exploited here to study exclusively the transition conditions. The wave propagation is highly dependent on the transition conditions. It is shown that a small change in the spring constants results in a large fluctuation in the reflection of the waves.

References

[1] N.J. Balmforth, and R.V. Craster, Ocean Waves and Ice Sheets, *J. Fluid Mech.* **395** (1999) 89–124.

[2] H. Chung and C.M. Linton, Interaction between water waves and elastic plates: Using the residue calculus technique. *18th International Workshop On Water Waves and Floating Bodies*, Le Croisic, France, April, 2003.

[3] H. Chung and C. Fox, Propagation of Flexural Waves at the Interface Between Floating Plates. *International Journal of Offshore and Polar Engineering* **12** (2002) 163–170.

[4] D.V. Evans and T.V. Davies, *Wave-Ice Interaction Report 1313.* Hoboken: Davidson Laboratory, Stevens Institute of Technology 1968.

[5] D.V. Evans and R. Porter, Wave Scattering by Narrow Cracks in Ice Sheets Floating on Water of Finite Depth. *J. Fluid Mech.* **484** (2003) 143–166.

[6] C. Fox and H. Chung, *Harmonic Deflections of an Infinite Floating Plate.* Department of Mathematics, University of Auckland, Report Series **485** (2002).

[7] L.A. Tkacheva, Diffraction of surface waves at floating elastic plate. *17th International Workshop On Water Waves and Floating Bodies* Peterhouse, Cambridge, UK, April 2002.